LA-UR-16-27463

Title: Report on Concepts & Approaches for SSBD for eCHEM

Author(s): Murphy, Chantell Lynne-Marie

Intended for: Report

Issued: 2016-09-29

Report on Concepts & Approaches for SSBD for eCHEM

Chantell L. Murphy

September 28, 2016

1 Introduction

The verification of special nuclear material (SNM) in spent fuel pyroprocessing is an important safeguards challenge. The detection of spontaneous fission (SF) neutrons from curium is an accepted, non-destructive technique that has been applied to verify special nuclear material (SNM) content in used fuel and other materials in the fuel cycle. The nuclear material accounting (NMA) technique at the Korea Atomic Energy Research Institute's Reference Engineering-scale Pyroprocessing Facility (REPF) is based on the Cm balance technique[1]. The ^{244}Cm isotope is used as a Pu indicator because it is the dominant source of SF neutrons in the used fuel. The plutonium content in spent fuel can be obtained by multiplying the doubles (D) or singles (S) neutron count of spent fuel by the Pu/Cm ratio. Using D's is preferred to avoid the effect of neutrons produced from the (α,n) reactions; however in metal samples, (α,n) neutrons should be negligible. The Pu/Cm ratio can be determined by destructive analysis (DA) of small samples taken from the feed materials, the electrolyte, or the cathode deposit. Although DA is accurate, it is a more expensive and timely technique, but it is used to verify the results of nondestructive analysis (NDA) that would be done more frequently and easily[2].

This neutron counting technique can only be applied when curium and plutonium are not separated in the system and under normal operating conditions transuranics (TRU) are not separated in the pyroprocessing facility. The electrorefiner (ER) poses particular safeguards concerns and should be closely monitored using real time or near real time analysis (NRTA). While Pu and Cm exhibit similar electrochemical behavior

[3, 4], previous studies have shown that certain off-normal operating conditions in the ER may lead to the co-deposition of Pu on the cathode causing it to separate from the other TRUs[5, 6, 7].

Several publications have demonstrated the safeguards benefit from using process monitoring (PM) on nuclear facilities as a complementary measure to NMA[8, 9, 10, 11]. More recently, this concept was expanded and preliminarily demonstrated for pyroprocessing. The concept of Signature Based Safeguards (SBS) is part of this expansion and is built around the interpretation of input from various sensors in a declared facility coupled with complementary NMA methods to increase confidence and lower standard error inventory differences (SEID)[12, 13, 6]. The SBS methodology was conceptually developed and relies on NRTA of process monitoring data to detect material diversion complimented by robust containment and surveillance (C/S) measures. This work demonstrates one example of how the SBS framework can be used in the ER. In this SBS application, a combination of cyclic voltammetry (CV) and neutron counting is applied to track and monitor Pu mass balance.

2 Background

In electrorefining, the difference between normal and off-normal operations is based on the composition of the cathode. Normal operations result in a 100% pure U metal deposit, while off-normal operations result in significant contamination from Pu deposition on the cathode. This work further enhances SBS development for the electrorefiner by simulating off-normal events caused by changes in electrolyte concentration and using CV and neutron counting to identify them in process as opposed to at the end of the mass balance period.

Electrochemical sensors are very popular options for monitoring molten salts, since there are numerous electro-active species in a typical molten salt bath mixture of interest and both identification and quantification of these species is possible. The voltammetry probe is a set of three electrodes that are immersed into the salt bath specifically for the purpose of making an electrochemical measurement that provides some information about the electrolyte. Three voltammetry techniques are commonly used, Cyclic Voltammetry (CV), Pulse Voltammetry (PV), and Open Circuit Voltammetry (OCP).

The focus of this analysis is on CV, which is an electrochemical technique that scans a certain range of voltages back and forth. Within this range, the current generated is measured and plotted versus potential. Cyclic voltammetry has variables of scan rate, concentration, area of electrodes, and diffusion coefficient. When the scan rate, area of electrodes, and diffusion coefficient are fixed in the system, the current information can reflect the concentration of input elements. The limit of detection is approximately 0.1 wt. % based on the comparison between peak current and background current.

For illustrative purposes, figure 1 depicts CVs for a LiCl−KCl−$ThCl_4$ electrolyte at 500°C (773 K) at a scan rate of 50 mV/s for three different concentrations of $ThCl_4$. This plot was generated from electrochemical experiments conducted at the University of Utah's Metallurgy Department's Laboratory in 2015 using NOVA software[14]. $ThCl_4$ was used in this particular experiment to see how the CV responds to changes in concentration in the electrolyte, which relates to the current study looking at how Pu concentration changes in the electrolyte. The working electrode was scanned between two potentials. A potentiostat records the current that flows through the cell as a function of potential. The potential is defined as that of the working electrode minus that of a stable reference electrode. For these experiments, the reference electrode was Ag/AgCl encased in a thin mullite tube.

Figure 1: Cyclic voltammograms at 50 mV/s of LiCl−KCl−$ThCl_4$ at 773 K

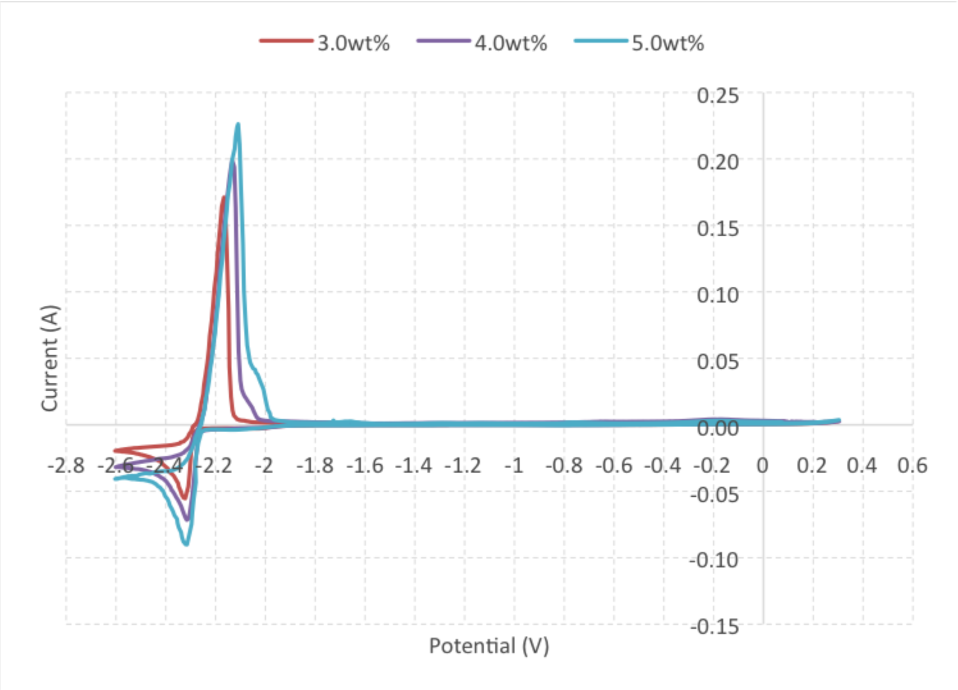

The peak at -2.35 V (vs. Ag/AgCl) is the reduction peak for Th(IV)/Th(0), and the peak at -2.18 is the oxidation peak. It can be seen that as the concentration of $ThCl_4$ increases in the electrolyte, the current also increases.

In addition to small scale concentration change experiments, computational modeling of the ER is also being conducted. A 1-dimensional transient electrorefiner model called Enhanced REFIN with Anodic Dissolution (ERAD) is being used to investigate various off-normal operating conditions. ERAD is a Fortran code that was developed to model mass transport and separation in the electrorefiner[15]. Most recently it was used simulate running the ER continuously for several cycles without cleaning the electrolyte[16]. ERAD ran for four different currents (measured in amperes (A)) with each cycle lasting 24 hours, see Table 1:

Table 1: Model current and associated number of cycles

Current (A)	Cycles
15	365
50	295
100	63
150	38

The same input for the anode was used for each run with concentrations of U, Pu, and Cm set to 98.0 wt.%, 1.0 wt.%, and 0.01 wt.% respectively. Running in this manner loosely resembles how a fresh batch of spent fuel would be added to the ER, however the ERAD simulation only uses 10 elements and not all the elements found in a spent fuel bundle. The same input was also used for the cathode for each run, simulating the cathode being cleaned after each run. However the electrolyte concentration changed with each run. A bash script was written in order to take the last line of the electrolyte concentration output file for each run and automatically insert it into the new input file for the next run simulating the electrolyte not being cleaned, potentially due to a failure in the salt cleanup operation. The purpose was to see when the Pu/Cm ratio changes in the electrolyte. The ERAD results are shown in Figure 2.

Depending on the current, the ratio remains constant for several cycles without any salt cleanup. The Pu/Cm ratio remains constant at 15 A. The ratio changes at cycle 157 at 50 A. For higher currents the Pu/Cm ratio changes much sooner. At 100 A, the ratio changes at cycle 37. At 150 A, the ratio changes at cycle 7.

The change in Pu/Cm is due to the off-normal condition of Pu electrodepositing on

Figure 2: Semi-log graph of plutonium to curium ratio in electrolyte

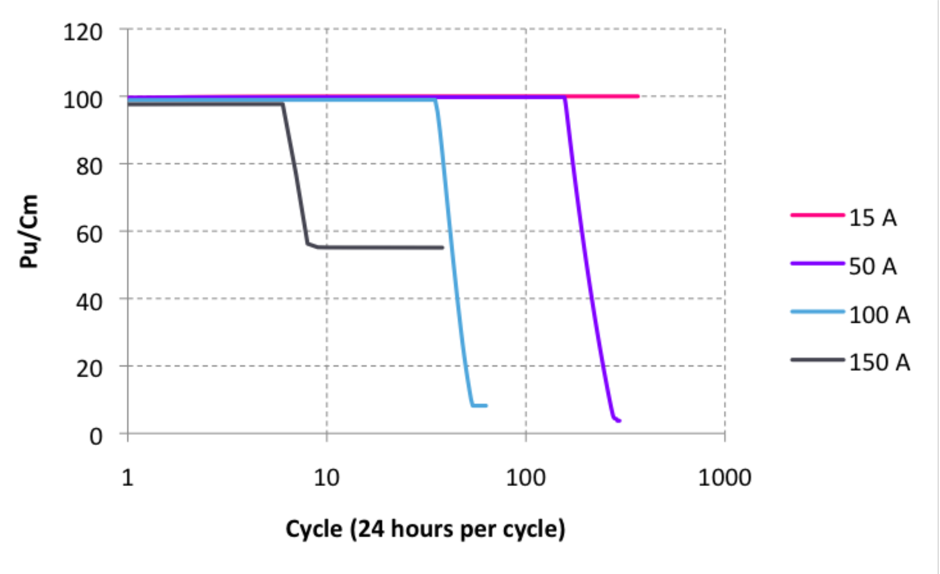

the cathode. This occurs when the U concentration becomes low enough to change the potential. The U concentration decreases in the electrolyte as it is being reduced onto the cathode and removed after each run. Meanwhile, both Pu and Cm are continuously increasing in the electrolyte as they are oxidized from the anode into the electrolyte.

It is important to understand this process through the use and relationship of electrochemical PM and NDA techniques. Knowing how to interpret CV responses, for example when Pu electrodeposits, and the relationship with neutron counting will enable a valuable implementation for a SBS component.

3 Experiment Concept

Small scale experiments will be conducted in an electrochemical cell to simulate the behavior of U, Pu, and Cm in the electrorefiner in order to create the off-normal condition of Pu depositing on the cathode. The goal will be to obtain cyclic voltammetry (CV) data and conduct DA using inductively coupled plasma mass spectrometry (ICP-MS) on samples taken from the electrolyte and cathode deposits under different concentration profiles. The ICP-MS concentration data will be used as a surrogate for neutron counting.

Due to such low concentrations of Cm in the electrolyte, CV might not register the presence of Cm but it will register Pu and changes in Pu concentration. When coupled with neutron counting for verifying Cm, the two techniques may reveal patterns that will support the SBS technique making Pu tracking more efficient.

With each run, the U concentration in the electrolyte decreases because it is being deposited on the cathode and removed from the ER salt bath. Meanwhile with each run, both $PuCl_3$ and $CmCl_3$ concentrations are increasing in the electrolyte at a steady rate as they are being oxidized from the anode. If the electrolyte is not cleaned and UCl_3 concentration continues to decrease, the potential drops and the Pu starts to reduce and deposit onto the cathode.

In the small scale experiment, U, Pu and Cm will not be used due to radioactivity. Tb, Mg, and Gd will be used to replaces U, Pu and Cm respectively. The surrogates were chosen due the difference in standard potential, E measured in volts (V). Table 2 shows the potentials and the differences for the spent fuel elements under investigation and their surrogates[17, 3, 4, 18, 19, 20].

Table 2: Standard potentials and differences for elements under investigation

E(V)		
U	-2.412	$\Delta E_{U,Pu} = 0.307$ $\Delta E_{Pu,Cm} = 0.0.081$
Pu	-2.719	
Cm	-2.8	

(a) Spent fuel elements

E(V)		
Tb	-2.3	$\Delta E_{Tb,Mg} = 0.378$ $\Delta E_{Mg,Gd} = 0.15$
Mg	-2.678	
Gd	-2.828	

(b) Experimental surrogate elements

The experimental electrochemical runs will consist of normal and off-normal operations. The first seven runs will simulate the normal operation where $TbCl_3$ is reacting with Mg and Gd. The reactions are as follows:

$$\begin{aligned} 2\,\mathrm{TbCl_3} + 3\,\mathrm{Mg^{2+}} &\longrightarrow 3\,\mathrm{MgCl_2} + 2\,\mathrm{Tb^{3+}} \\ \mathrm{TbCl_3} + \mathrm{Gd^{3+}} &\longrightarrow \mathrm{GdCl_3} + \mathrm{Tb^{3+}} \end{aligned} \tag{1}$$

Once $MgCl_2$ accumulates in the electrolyte, the off-normal operating conditions will lead to Mg electrodepositing on the cathode with the following reactions:

$$\begin{aligned} 3\,\mathrm{MgCl_2} + 2\,\mathrm{Gd^{3+}} &\longrightarrow 2\,\mathrm{GdCl_3} + 3\,\mathrm{Mg^{3+}} \\ 3\,\mathrm{MgCl_2} + 2\,\mathrm{Tb^{3+}} &\longrightarrow 2\,\mathrm{TbCl_3} + 3\,\mathrm{Mg^{3+}} \end{aligned} \tag{2}$$

The amount of material electrolyzed per run were calculated from the reaction equations above. The results are displayed in Figure 3 and the calculated Mg/Gd ratio is displayed in Figure 4, both calculated from equations 1 and 2.

Figure 3: Calculated Tb, Mg, and Gd concentrations in electrolyte

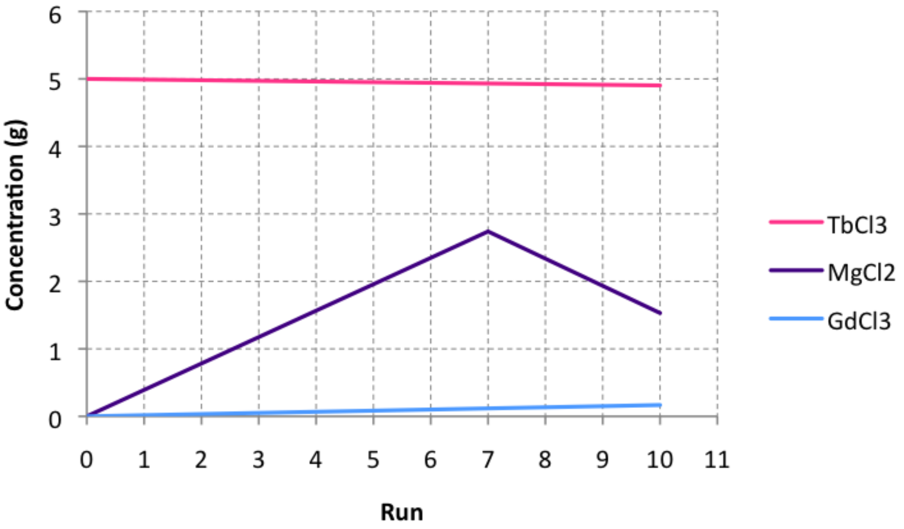

Figure 4: Calculated Mg/Gd ratio in electrolyte

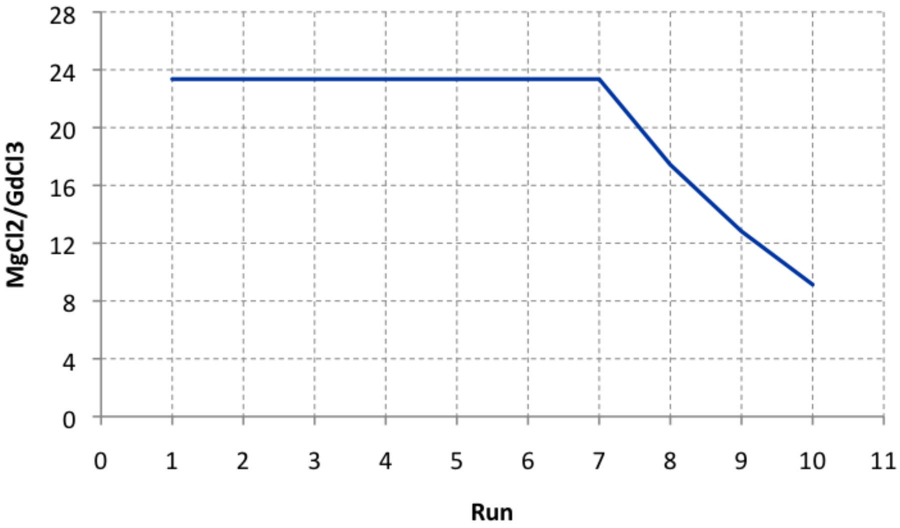

The trends in these figures resemble the ERAD results from the U, Pu, and Cm runs.

3.1 Setup

Electrochemical experiments will be conducted at the University of Utah's Metallurgy Department's Laboratory. The experiments will be performed in an argon gas atmosphere glove box that contains a Kerr Auto-Electro Melt Furnace, which operates at temperatures of 600 - 800K. The experiment requires an alumina crucible able to fit in the furnace with a lid able to hold three electrodes that will move in and out of the well. The anode contains a stainless steel basket of Tb, Mg, and Gd metals. The cathode is a stainless steel rod. Tungsten rods will be used in between each run to take CVs. Data will be collected using NOVA Software. The reference electrode is a Ag/AgCl mixture contained in a mullite tube. The electrolyte for the experiments consists of $LiCl-KCl-TbCl_3$. A picture of a similar three electrode setup is depicted in figure 5.

Figure 5: Example of electrochemical experiment setup

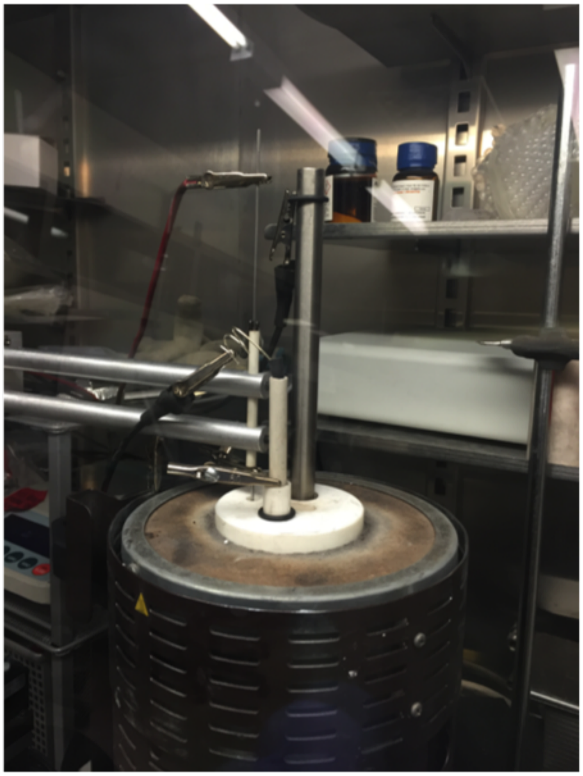

In preparation for the experiment a number of parameters will be determined. CV runs will be conducted to evaluate the reduction potential (vs. Ag/AgCl reference electrode) for Tb and Mg. Runs will be conducted to determine the limiting current for Tb deposition and for Tb and Mg codeposition. The electrolyte to accomplish these baseline tests will consist of $LiCl-KCl-TbCl_3-MgCl_2-GdCl_3$ and the working electrode will be a W rod.

Once the potential and currents are determined, the experimental runs will be conducted and compared to the simulated ERAD results. The anode basket will contain Tb, Mg, and Gd metal powders. The electrolyte will consist of $LiCl-KCl-TbCl_3$. As seen in Figure 3, $TbCl_3$ only decreases by a small amount per run. This is because it will be necessary to add a small amount before each run in order to prevent it from all being electrolyzed before the end of the experiment. According to the reaction calculations, about 30 g of $TbCl_3$ will be needed in order to sustain 10 cycles. Unfortunately starting with 30 g of $TbCl_3$ will make it difficult if not impossible to melt the electrolyte completely. To mitigate complications, 5 g will be used in the first run and 1.638 g of $TbCl_3$ will be added to the electrolyte before each subsequent run, using a total of approximately 22 g of $TbCl_3$. Each run will result in CV data and samples extracted from the electrolyte and cathode for ICP-MS analysis. The electrolyte samples will confirm how much Gd, Mg and Tb are in the electrolyte between each run, which will be compared with the theoretical calculations. The cathode samples will confirm how much Tb and Mg is deposited.

Table 3 shows the test matrix of data that will be collected for this set of experiments. The CV data and ICP-MS data will be collected in separate files and then aggregated for final analysis.

Table 3: Test Matrix

Run	Time (s)	Current (A)	CV data	ICP-MS data
1				
2				
3				
5				
6				
7				
8				
9				
10				

3.1.1 Materials

Table 4 lists all the materials needed to collect the baseline data and conduct the experimental runs.

Table 4: Experiment materials and amounts needed

Material	Amount
$LiCl-KCl$	50 g
$TbCl_3$	25 g
$MgCl_2$	1 g
$GdCl_3$	1 g
Terbium metal powder	1 g
Magnesium metal powder	0.1 g
Gadolinium metal powder	0.01 g
$AgCl$	5 g
Silver wire	1
Mullite Tubes	1
Tungsten rods	10
Stainless steel rods	20
Stainless steel baskets	10
Alumina crucible	1

Stainless steel rods and baskets will need to be machined to serve as the anode. The basket will hold the Tb, Mg, and Gd metal powders that will be lowered into the molten salt bath in order to react with the $TbCl_3$. A drawing of the anode design is shown in Figure 6.

Figure 6: Mechanical drawing of stainless steel anode basket design

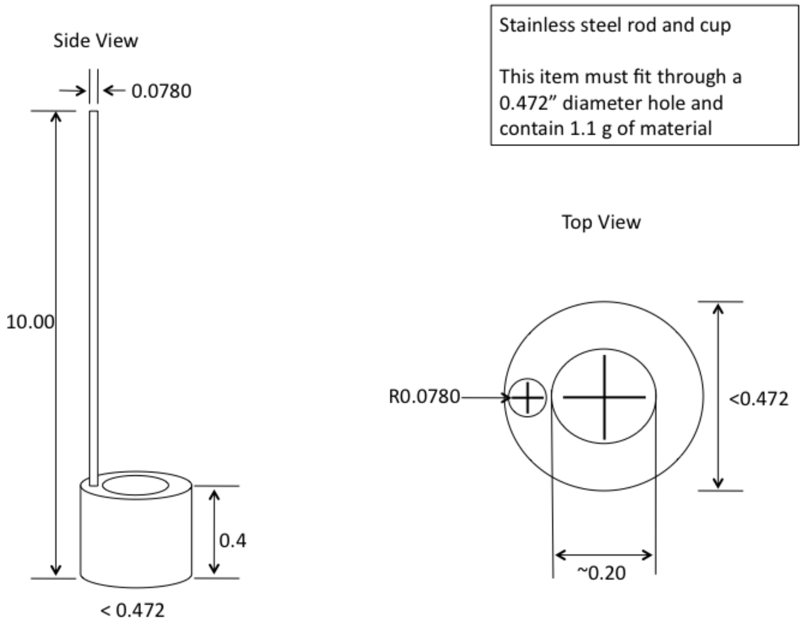

Stainless steel rod and cup

This item must fit through a 0.472” diameter hole and contain 1.1 g of material

4 Discussion

The main purpose of this experiment is to determine if meaningful information can be gained from CV measurements with regard to the Mg/Gd ratio. This data will be coupled with ICP-MS to verify Gd concentrations and analyzed for statistical significance. It is expected the CV data will register a significant change under the off-normal operating conditions. Knowing how to identify and interpret those changes may help inform how to target more traditional neutron counting methods, which could support a more efficient safeguards system. The experimental results will be compared with theoretical calculations and the ERAD simulations.

References

[1] T.-H. Lee, Y.-S. Kim, T.-J. Kwon, H.-S. Shin, and H.-D. Kim, "Determination of the plutonium mass and curium ratio of spent fuel assemblies for input nuclear material accountancy of pyroprocessing, and analysis of their errors," *Nuclear Technology*, vol. 179, pp. 196–204, August 2012.

[2] N. Miura and H. Menlove, "The use of curium neutrons to verify plutonium in spent fuel and reprocessing wastes," Report LA-12774-MS, Los Alamos National Laboratory, 1994.

[3] J. Serp, R. Konings, R. Malmbeck, J. Rebizant, C. Scheppler, and J.-P. Glatz, "Electrochemical behaviour of plutonium ion in licl–kcl eutectic melts," *Journal of Electroanalytical Chemistry*, vol. 561, no. 1, pp. 143–148, 2004.

[4] A. Osipenko, A. Maershin, V. Smolenski, A. Novoselova, M. Kormilitsyn, and A. Bychkov, "Electrochemical behaviour of curium(iii) ions in fused 3licl–2kcl eutectic," *Journal of Electroanalytical Chemistry*, vol. 651, no. 1, pp. 67–71, 2011.

[5] R. Hoover, P. Lafreniere, and E. Blandford, "Commercial-scale pyroprocessing failure modes and implications for operations and safeguards," in *Transactions of the American Nuclear Society*, vol. 110, pp. 58–61, 2014.

[6] P. L. Lafreniere, D. S. Rappleye, R. O. Hoover, M. F. Simpson, and E. D. Blandford, "Demonstration of signature-based safeguards for pyroprocessing as

applied to electrorefining and the ingot casting process," *Nuclear Technology*, vol. 189, pp. 173–185, February 2015.

[7] M. Gonzalez, L. Hansen, D. Rappleye, R. Cumberland, and M. F. Simpson, "Application of a one-dimensional transient electrorefiner model to predict partitioning of plutonium from curium in a pyrochemical spent fuel treatment process," *Nuclear Technology*, vol. 192, pp. 165–171, November 2015.

[8] T. Burr, K. B. Sylvester, K. Myers, S. Demuth, A. Bakel, J. Krebs, S. Bryan;, C. Orton, M. Ehinger, H. Garcia, J. Howell, S. Johnson, M. Thomas, and J. Damico, "Roles for process monitoring in nuclear safeguards at aqueous reprocessing plants," *Journal of Nuclear Materials Management*, vol. XL, no. 2, pp. 42–52, 2012.

[9] H. E. Garcia, M. F. Simpson, W.-C. Lin, T.-S. Yoo, and R. B. Carlson, "Detecting proliferation activities via system-centric integration and interpretation of multimodal data collected from a system of sensors," in *Institute of Nuclear Materials Management 54th Annual Meeting Proceedings*, 2013.

[10] H. E. Garcia, W. Lin, S. Johnson, T. Burr, S. Demuth, A. Bakel, J. Krebs, and M. Ehinger, "Integrated process monitoring based on systems of sensors for enhanced nuclear safeguards sensitivity and robustness," in *Institute of Nuclear Materials Management 52nd Annual Meeting Proceedings*, 2011.

[11] B. B. Cipiti, F. A. Durán, B. Key, Y. Liu, I. Lozano, and R. Ward, "Modeling and design of integrated safeguards and security for an electrochemical reprocessing facility," tech. rep., Sandia National Laboratories, 2012.

[12] R. Wigeland, T. Bjornard, and B. Castle, "The concept of goals-driven safeguards," tech. rep., Idaho National Laboratory, 2009.

[13] M. F. Simpson, "Developments of spent nuclear fuel pyroprocessing technology at idaho national laboratory," tech. rep., Idaho National Laboratory, March 2012.

[14] A. NOVA, "Nova advanced electrochemical software," September 2016.

[15] R. M. Cumberland and M.-S. Yim, "Development of a 1d transient electrorefiner model for pyroprocess simulation," *Annals of Nuclear Energy*, vol. 71, p. 52–59, September 2014.

[16] C. Murphy, P. Lafreniere, E. Arthur, M. F. Simpson, and E. D. Blandford, "Effects of salt cleanup failure modes on the electrorefiner in a signature based safeguards (sbs) framework," in *INMM 57th Annual Meeting*, July 2016.

[17] O. Shirai, T. Iwai, Y. Suzuki, Y. Sakamura, and H. Tanaka, "Electrochemical behavior of actinide ions in licl–kcl eutectic melts," *Journal of Alloys and Compounds*, vol. 271–273, pp. 685 – 688, 1998.

[18] M. Bermejo, J. Gómez, A. Martínez, E. Barrado, and Y. Castrillejo, "Electrochemistry of terbium in the eutectic licl–kcl," *Electrochimica Acta*, vol. 53, no. 16, pp. 5106 – 5112, 2008.

[19] T. Hao, Y. Yong-De, Z. Mi-Lin, X. Yun, Z. Zhi-Jian, D. Wei-Chao, and H. Hui, "Electrochemistry of mgcl2 in licl-kcl eutectic melts," *ACTA PHYSICO-CHIMICA SINICA*, vol. 29, no. 8, pp. 1698–1704, 2013.

[20] C. Caravaca, G. de Córdoba, M. Tomás, and M. Rosado, "Electrochemical behaviour of gadolinium ion in molten licl–kcl eutectic," *Journal of Nuclear Materials*, vol. 360, no. 1, pp. 25 – 31, 2007. Proceedings has been selectedProceedings of the Seventh International Symposium on Molten Salts Chemistry and Technology (MS7 – Session 6: Workshop on Nuclear Energy and Nuclear Wastes.